A Task-Agnostic Hip Exoskeleton for Osteoarthritis Pain Relief: Energetic Control Across Activities of Daily Life

Jiefu Zhang, Nikhil V. Divekar, Ernesto Hernandez Hinojosa, and Robert D. Gregg

***Abstract*— Hip osteoarthritis (OA) affects millions worldwide, yet effective conservative (non-surgical) treatments are still limited. Conventional hip braces cannot reduce painful joint loads associated with contractile forces from flexors and extensors during locomotion. Powered hip exoskeletons could potentially reduce biological hip moments by applying flexion/extension torques, thus attenuating muscle forces that contribute to OA pain. Here, we present a novel task-agnostic controller for a backdrivable hip exoskeleton that relieves hip OA pain across the primary activities of daily life. Inspired by the energy shaping method, this controller utilizes biomechanics-based components to assist with level walking, ramp and stairs ascent/descent, and sit-to-stand transitions, which can be customized to different populations, like hip OA. In a pilot study with three hip OA participants, the hip exoskeleton holistically reduced pain and perceived difficulty during a multi-activity test (except difficulty of level walking). The exoskeleton also increased hip range of motion during walking, with subject-specific improvements in walking speed. This pilot study suggests that hip exoskeletons may offer a promising new intervention for managing hip OA.**

I. Introduction

Hip osteoarthritis (OA) is a degenerative joint disease that affects millions worldwide, yet effective conservative treatments are still limited. While total hip arthroplasty (THA) is considered the gold standard for late-stage hip OA patients, it is economically unjustifiable for less severe cases [1]. Pharmacologic treatments such as non-steroidal anti-inflammatory drugs (NSAIDs) [2] and intra-articular injection [3] are common treatments for mild OA. However, prolonged use of NSAIDS can have adverse effects [2], and masking pain without addressing root causes can result in further joint damage [4]. Exercise is typically recommended to counter muscle atrophy/dysfunction [5] that contributes to abnormal joint loading and pain [6]–[8]. However, pain often forces patients to avoid strenuous activities like stair climbing and limit themselves to low-impact exercises like walking. Restricted mobility can perpetuate a detrimental cycle where muscle weakness and physical inactivity contribute to the worsening of OA symptoms [9].

Hip unloading braces can reduce pain caused by hip OA by restricting frontal plane motions and thus reducing hip joint load [10], [11], but their effectiveness was subject-dependent. This can be potentially attributed to the bulkiness and rigidity of current braces, which are essential for motion restriction but negatively affect their usability [12]. Moreover, they neglect flexion/extension moments that also cause OA pain [13], since unloading forces by restricting motion in the sagittal plane is not an option, given the necessary range of motion (RoM) for locomotion.

Powered exoskeletons, which apply external torque to joints, offer a promising approach to reduce joint compression forces [14] and associated pain in lower-limb OA. These devices have been shown to effectively decrease joint moments [15] and muscle effort [16] during various activities. Since joint compression forces during dynamic movements are primarily caused by muscle contractions generating internal joint moments [17], powered exoskeletons can potentially benefit OA patients by providing external torques that partially reduce the requisite muscle activation. Simulation studies [14] have suggested that knee exoskeletons applying pure torque can decrease joint loading across different walking speeds. However, the effects of hip exoskeletons on OA patients remain to be investigated.

In order for hip exoskeletons to help manage OA pain on a daily basis, they must be sufficiently versatile to support the various activities of daily life (ADLs). However, existing commercial hip exoskeletons like Samsung GEMS [18], [19] typically use task-specific controllers that must first identify the activity being performed before applying pre-programmed torque profiles. This approach proves problematic in real-world applications due to the unpredictable and varied nature of daily activities. For instance, studies with the highly-geared Keeogo knee exoskeleton [20] failed to show immediate improvements for knee OA patients, likely due to the lengthy user adaptation needed to effectively use the task recognition-based controller. While neural networks trained with unimpaired human data can enhance task adaptability by estimating normative biological hip moments across various activities [15] (referred to as a *task-agnostic* controller), the lack of tunability limits customization for specific patient populations like hip OA. Moreover, the "black box" nature of neural networks raises safety concerns when used with impaired populations due to the possibility of unpredictable behavior outside training scenarios.

Our previous research on energy shaping-based controllers has shown promise in providing task-agnostic, biomimetic torque assistance with improved safety and stability guarantees [21]–[24]. However, the optimization over hundreds of non-intuitive torque bases made these methods susceptible to over-fitting the training data and impractical to tune for more effective assistance, resulting in limited interpretability

This work was supported by the National Institute of Biomedical Imaging and Bioengineering of the NIH under Award Number R01EB031166. The content is solely the responsibility of the authors and does not necessarily represent the official views of the NIH.

The authors are with the Department of Robotics, University of Michigan, Ann Arbor, MI 48109, USA. Corresponding author: Robert D. Gregg. Contact: {zjiefu, ndivekar, ehdz, rdgregg}@umich.edu

and customizability. In [25], an energy shaping controller was designed using physically-meaningful components like virtual springs and dampers, which are inherently passive and intuitive but not necessarily biomimetic. This idea was extended in [16] by optimizing physically-meaningful energetic components to match human data followed by manual tuning to maximize quadriceps assistance during lifting, lowering, and carrying tasks. By moving away from purely data-driven optimization of abstract torque bases, this approach has demonstrated superior effectiveness in improving physical performance and reducing muscle effort across various activities while maintaining customizability. The use of intuitive parameters also makes the controller more practical to tune and adapt for individual needs. While the results in [16] are promising for healthy individuals, this technology may also have impact for people with hip OA.

In this paper, we designed and implemented an energy shaping-inspired hip exoskeleton controller based on the approach in [16] for individuals with hip OA. Fig. 1 provides a high-level overview of our controller, which utilizes virtual springs modulated by kinematic variables such as joint angles and velocities, featuring physically-meaningful parameters that can be customized. This design represents our first key contribution, offering task-agnostic assistance for common ADLs with improved interpretability and customizability. Our second major contribution lies in investigating the effects of powered hip exoskeleton assistance on the hip OA population, hypothesizing that it could reduce pain and decrease the difficulty of performing ADLs. To validate this, three participants with hip OA performed various activities both with and without our hip exoskeleton at different assistance levels. Results demonstrated significant pain and difficulty reductions during hip-intensive tasks across all subjects, along with subject-specific improvements in walking speed accompanied by increased hip RoM. These promising outcomes reveal the potential of powered hip exoskeletons as an effective treatment option for individuals with hip OA.

II. Controller Design and Implementation

In our previous hip exoskeleton controller design [23], assistive torque was formulated as a linear combination of trigonometric basis functions, whose coefficients were determined through off-line optimization using normative human data. This approach presents challenges for impaired populations like hip OA patients, primarily due to its heavy dependence on data and the use of non-intuitive basis functions. Designing controllers for impaired populations is complicated by the scarcity of rich population-specific datasets, leading to the use of datasets with less subjects and activities, thus increasing the risk of overfitting. Furthermore, patient datasets often consist of pathological movement patterns, which will be reproduced by a purely data-driven controller, leading to suboptimal assistance. For example, hip OA patients typically exhibit reduced range of motion during walking, partly stemming from insufficient hip extension moment [8]. A controller developed using such patient data would reproduce these limited movement patterns, resulting in insufficient torque. Unintuitive control parameters would also prevent heuristic fine-tuning based on user feedback, often essential in clinical settings. To address these limitations, in this paper we propose a biomechanics-informed controller, which incorporates virtual springs modulated by human kinematics. This new design can provide task-agnostic assistance for hip OA patients, while remaining tunable.

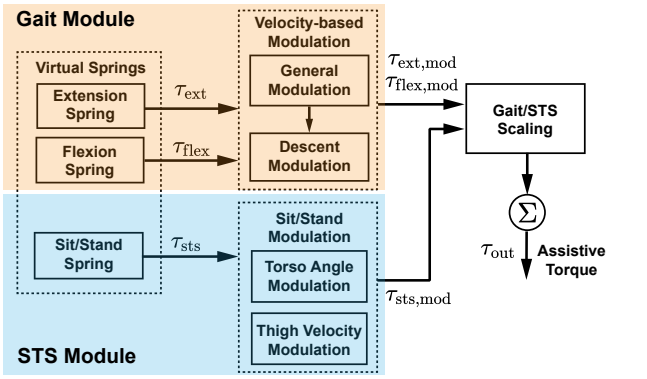

Fig. 1. High-level overview of the controller. Torque generated by virtual springs is modulated based on joint kinematics, and then scaled and summed to obtain the output assistive torque.

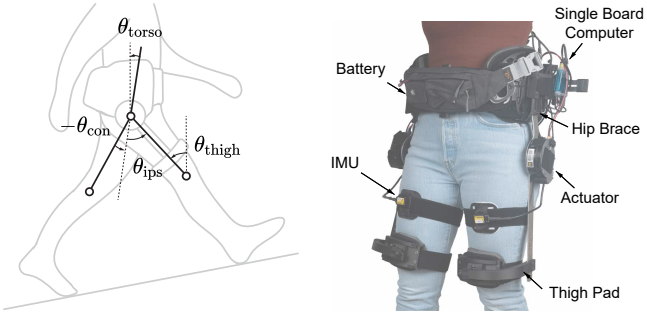

Fig. 2. **Left:** Definitions of angles used in the controller. Black-outlined circles represent the centers of hip and knee joints. $\theta_{\text{torso}}, \theta_{\text{thigh}}, \theta_{\text{ips}}$, and θ_{con} denote torso angle, thigh angle, ipsilateral hip angle, and contralateral hip angle respectively. **Right:** Picture of the modified M-BLUE hip module. For clarity only one of the inertia measurement units (IMUs), actuators, and thigh pads are labeled.

A. Physical Component-based Controller Design

The physical component-based controller comprises two modules: the gait module that generates torque for gait activities (level walking, ramp and stairs ascent/descent), and the sitting/standing (STS) module that generates torque for sit-to-stand transitions. The gait module includes two unidirectional virtual torsion springs—the extension spring and the flexion spring, modulated by joint velocity. The STS module consists of one unidirectional virtual torsion spring—the STS spring, modulated by the torso angle and thigh velocity. The torque from the two modules is scaled and combined to provide the output assistive torque. The definition of joint angles used in the controller is shown in Fig. 2 (left). The counterclockwise (flexion) direction is defined as positive.

1) Gait Module: In the gait module, the extension spring and flexion spring provide extension and flexion torque

during gait activities. The torques generated by the two springs are given by

$$\begin{aligned}\tau_{\text{ext}} &= \min\left(0,\ k_{\text{ext}} \cdot (\theta_{\text{ips}} - \theta_{\text{ext,eq}})\right) \\ \tau_{\text{flex}} &= \max\left(0,\ k_{\text{flex}} \cdot (\theta_{\text{flex,eq}} - \theta_{\text{ips}})\right),\end{aligned} \tag{1}$$

where $k_{\text{ext}},\ k_{\text{flex}}$ are the constant spring stiffness values of the extension and flexion springs, θ_{ips} is the ipsilateral hip angle, and $\theta_{\text{ext,eq}}$, $\theta_{\text{flex,eq}}$ are the equilibrium angles of extension and flexion springs respectively. The $\min(\cdot)$ and $\max(\cdot)$ functions ensure that springs are unidirectional and only provide torque in the intended direction.

We want to predict biomimetic torques using measurable input kinematics (e.g., angles and velocities) across multiple ADLs, which is not feasible with virtual springs alone, since similar hip angles may correspond to dissimilar biological hip moments in different activities and gait phases. For example, a vertical thigh orientation during mid-stance and mid-swing corresponds to conflicting extension and flexion biological moments, respectively. Prediction power can be substantially improved by modulating the torque from two springs using joint velocity (the general modulation block in Fig. 1). In early-to-mid stance, the flexion spring torque is attenuated due to large negative hip velocity, providing extension torque aligned with leg movement. This attenuation continues until late stance, when hip velocity is slightly negative, signaling the need for overall negative power for braking. Similarly, in early-to-mid swing, the extension spring torque is attenuated based on large positive hip velocity until late swing. This velocity-based modulation strategy for general gait activities enables precise control of torque application timing across gait phases. Due to the smoothness and boundedness of sigmoid function, we chose it as the nonlinear modulation function:

$$\sigma(x, w, \phi) = \frac{1}{1 + e^{-w \cdot x + \phi}}\ , \tag{2}$$

where x is the input argument, and w, ϕ are parameters that determine the slope and horizontal shifts of the sigmoid function. Let x be the angular velocity $\dot{\theta}$, then (2) maps $\dot{\theta} \in \mathbb{R}$ to $[0, 1]$, ensuring the boundedness of the modulation. By adjusting w and ϕ, the timing of assistive torque and its sensitivity to velocity can be tuned.

The general modulation factors can then be determined by

$$\begin{aligned}\eta_{\text{ext}} &= \sigma(\dot{\theta}_{\text{ips}}, w_{\text{ext}}, \phi_{\text{ext}})\ , \\ \eta_{\text{flex}} &= \sigma(\dot{\theta}_{\text{ips}}, w_{\text{flex}}, \phi_{\text{flex}})\ ,\end{aligned} \tag{3}$$

where $\dot{\theta}_{\text{ips}}$ is the ipsilateral hip angular velocity, and $w_{\text{ext}}, w_{\text{flex}}, \phi_{\text{ext}}, \phi_{\text{flex}}$ are parameters to be determined.

For certain descent tasks, such as stair descent, modulations solely based on velocity direction are insufficient to generate biomimetic assistive torque. During mid-swing, the concentric contraction of the hip flexors swings the leg forward. On the other hand, a hip flexion velocity is also observed during stance in descending tasks, associated with the eccentric contraction of hip extensors, to allow a "controlled lowering" of body center-of-mass. In this case, the exoskeleton needs to provide torque against the leg's motion to brace the user from collapsing, which is challenging with existing modulations since they tend to provide torque that aligns with the leg motion's direction (or sign of the velocity). By analyzing normative kinematics of descending tasks, we observed that during early to mid-stance, the ipsilateral hip flexes for lowering, while the contralateral hip flexes to swing the leg forward. This pattern allows us to further introduce descent modulation for effective assistance during descending tasks, determined by the descent modulation factor

$$\begin{aligned}\eta_{\text{desn}} = \sigma(\dot{\theta}_{\text{ips}}, w_{\text{ips}}, \phi_{\text{ips}}) \cdot \sigma(\dot{\theta}_{\text{con}}, w_{\text{con}}, \phi_{\text{con}}) \\ \cdot \text{step}(\theta_{\text{ips}} - \theta_{\text{con}} - \theta_{\text{th}})\end{aligned} \tag{4}$$

where $\dot{\theta}_{\text{con}}$ is the contralateral hip angular velocity, step$(\cdot)$ is the step function, θ_{con} is the contralateral hip angle, and θ_{th} is the angle difference limit. Parameters $w_{\text{ips}}, \phi_{\text{ips}}, w_{\text{con}}, \phi_{\text{con}}$ are designed such that both sigmoid functions converge to 1 when velocities are positive and to 0 when velocities are negative. The multiplication acts as a proxy of the "AND" logic operation, allowing $\eta_{\text{des}} \to 1$ only when both thighs are flexing, an indicator of descent activities. The step function further restricts the descent modulation to only be applied in a certain range of joint angle.

Combining (1), (3), and (4) gives the extension and flexion torques from the gait module:

$$\begin{aligned}\tau_{\text{ext,mod}} &= \tau_{\text{ext}} \cdot \left[\eta_{\text{desn}} \cdot C_{\text{ext}} + (1 - \eta_{\text{desn}}) \cdot \eta_{\text{ext}}\right]\ , \\ \tau_{\text{flex,mod}} &= \tau_{\text{flex}} \cdot \left[\eta_{\text{desn}} \cdot C_{\text{flex}} + (1 - \eta_{\text{desn}}) \cdot \eta_{\text{flex}}\right]\ ,\end{aligned} \tag{5}$$

where C_{ext} and C_{flex} are constant parameters to be chosen. General modulation and descent modulation together comprise velocity-based modulation, which changes the angle to torque mapping of extension and flexion springs to angle-velocity to torque, improving versatility and allowing more task-adaptive, biomimetic assistance from simple virtual springs.

2) STS Module: Due to the differences between sit-to-stand transitions and other walking tasks, the STS module is designed separately and operates in parallel with the gait module. The core of the STS module is the STS spring, a unidirectional virtual torsion spring with equilibrium angle at $\theta_{\text{thigh}} = 0°$, where θ_{thigh} is the ipsilateral thigh angle, as defined in Fig. 2. An extension restoring torque is generated when the thigh is flexed, determined by

$$\tau_{\text{sts}} = \min(0,\ -k_{\text{sts}} \cdot \theta_{\text{thigh}})\ . \tag{6}$$

Similar to the gait module, solely relying on the thigh angle leads to large extension torque at the end of the stand-to-sit transition and while seated. Therefore, to reduce torque while the user is seated, τ_{sts} is first modulated based on the torso angle θ_{torso}, as defined in Fig. 2 (left). The torso angle is a key differentiator between the sit-to-stand transition and a sitting posture, where the sit-to-stand transition exhibits an anterior torso lean ($\theta_{\text{torso}} > 0$). Furthermore, to reduce bracing during the late stand-to-sit transition, hip velocity is used to taper down extension torque when the thigh is flexing, indicating a stand-to-sit transition. Combining the

two modulations, the modulation factors for STS torque are determined by

$$\begin{aligned} \eta_{\text{sts,torso}} &= \sigma(\max(0, \theta_{\text{torso}}), w_{\text{torso}}, \phi_{\text{torso}}) \ , \\ \eta_{\text{sts,vel}} &= \sigma(\dot{\theta}_{\text{ips}}, w_{\text{vel}}, \phi_{\text{vel}}) \ . \end{aligned} \tag{7}$$

The maximum function $\max(0, \theta_{\text{torso}})$ allows the STS spring to only engage when $\theta_{\text{torso}} > 0$ (forward torso lean). Combing (6) and (7) gives the modulated STS torque:

$$\tau_{\text{sts,mod}} = \tau_{\text{sts}} \cdot \eta_{\text{sts,torso}} \cdot \eta_{\text{sts,vel}} \ .$$

3) Module Integration: To create seamless transitions between the gait module and the STS module, the torque from both modules is scaled based on the symmetry of bilateral kinematics, serving as a strong indicator of walking and STS activities. The scaling factor is determined by

$$\beta = \sigma(|\theta_{\text{ips}} - \theta_{\text{con}}|, w_{\text{sc}}, \phi_{\text{sc}}) \cdot \text{step}(|\dot{\theta}_{\text{ips}} - \dot{\theta}_{\text{con}}| - \omega_{\text{th}}) \ ,$$

where ω_{th} is the velocity difference limit. The step function ensures that β is nonzero only when the bilateral velocity is below the threshold determined by ω_{th}, implying symmetric bilateral velocities. By modifying $w_{\text{sc}}, \phi_{\text{sc}}$, and ω_{th}, one can adjust the sensitivity to asymmetry. Subsequently, the torques from the walking and STS modules are combined as a convex combination to produce the output torque

$$\tau_{\text{out}} = \beta \cdot \tau_{\text{sts,mod}} + (1 - \beta) \cdot (\tau_{\text{ext,mod}} + \tau_{\text{flex,mod}}) \ .$$

B. Parameter Optimization

Our biomechanics-informed design offers enhanced flexibility, enabling parameter adjustments beyond the original data-driven optimization process—a capability our previous design [23] lacked. Similarly to our previous work, we use normative datasets to inform the initial parameters (providing a *warm start*), which were later tuned based on pilot subject feedback. We formulate the parameter design problem as an optimization problem using normative human data from open-source multi-activity datasets [26] [27]. By minimizing the difference between estimated assistive torque (given normative input kinematics) and biological joint moment, we obtain parameters that serve as an improved starting point for further fine-tuning.

The parameters to be optimized are $w_{(\cdot)}, \phi_{(\cdot)}$ in (3), and $C_{\text{ext}}, C_{\text{flex}}$ in (5). The objective function is

$$\begin{aligned} J = \sum_{i \in T} \ & (\gamma_i \cdot \|\tau^i_{\text{out}} - \tau^i_{\text{bio}}\| + \gamma_2 \cdot \|\tau^0_{\text{out}}\| \\ & + \gamma_3 \cdot \|\text{sgn}(\tau^i_{\text{out}}) - \text{sgn}(\tau^i_{\text{bio}})\|) \ , \end{aligned}$$

where T is the set of activities used in the optimization, τ^i_{bio} is the scaled biological hip moment, and τ^i_{out} is the estimated assistive torque for activity i. The biological hip moment is scaled to 35% since the actuators can only provide around 1/3 of normative hip moment. τ^0_{out} denotes the estimated torque when all kinematics are zero, which corresponds to the configuration of standing still. $\text{sgn}(\cdot)$ is the sign function. γ_i is the task-dependent weight, and γ_2, γ_3 are constant weights. The first term of the objective function minimizes the difference between assistive torque and biological moment, with activity-dependent weight to emphasize hip demanding activities. The second term minimizes the static torque to prevent discomfort, and the third term minimizes the sign difference between τ^i_{out} and τ^i_{bio} to penalize assistive torque in the wrong direction.

To cover a range of ADLs, we used data from six subjects performing the following activities as our training set: level walking at 0.85 and 1.15 m/s, ascending and descending ramps at 5.2° and 11°, ascending and descending stairs with step heights of 5 and 7 inches (12.7 and 17.8 cm), and rising from a chair. The optimization problem was solved in MATLAB R2023b using the "`fmincon`" function, with physically reasonable lower and upper bounds. Figure 3 compares the estimated torque from the optimized controller, based on normative kinematics, to the corresponding scaled biological hip moment. Although data from healthy individuals were used, the optimized parameters served only as an initial guess and were further fine-tuned through feedback from pilot tests. Once determined, parameters remained fixed throughout the study.

C. Hardware Implementation

The controller was implemented on a bilateral hip exoskeleton shown in Fig. 2 (right), which is an improved hip module of the M-BLUE system [28]. The hip exoskeleton combines off-the-shelf hip braces (Breg T Scope Hip) with two highly backdrivable actuators (T-motor AK80-9 with Dephy FASTER driver) that provide 25 Nm peak torque with low reflected inertia (92.1 kg $\cdot$ cm^2). During the study, the maximum torque was limited to 20 Nm. Three IMUs (Microstrain 3DM-GX5 AHRS) were directly attached to thighs and torso to acquire: sagittal thigh, torso, and hip angles, and their angular velocities. The real-time controller ran on a Raspberry Pi 5 8 GB at 300 Hz. Hip angular velocity and commanded torque were filtered with second-order Butterworth low-pass filters with cutoff frequencies of 10 Hz and 5 Hz respectively. The system was powered by a 24 V, 2 Ah power tool battery (Kobalt 24-V Lithium Battery) and weighs approximately 4.3 kg. For safety, a remote e-stop switch was implemented to cut power to the motor if needed.

III. Hip Osteoarthritis Pilot Study

A. Experimental Design

To investigate the effect of the exoskeleton/controller on hip OA patients' physical performance and perceived pain and difficulty during different activities, we designed a study consisting of a multi-activity test approved by the Institutional Review Board at University of Michigan (HUM00201957). As a proof of concept, we enrolled three participants diagnosed with hip OA. Participant 1 was diagnosed with bilateral hip OA (S1: female, age-53, weight-52 kg, height-1.65 m), while participant 2 and 3 were diagnosed with unilateral hip OA (S2: male, age-32, weight-70 kg, height-1.71 m; S3: female, age-64, weight-78 kg, height-1.68 m). All participants gave written consent before participation. Participants were required to wear a safety harness to prevent falling during the study.

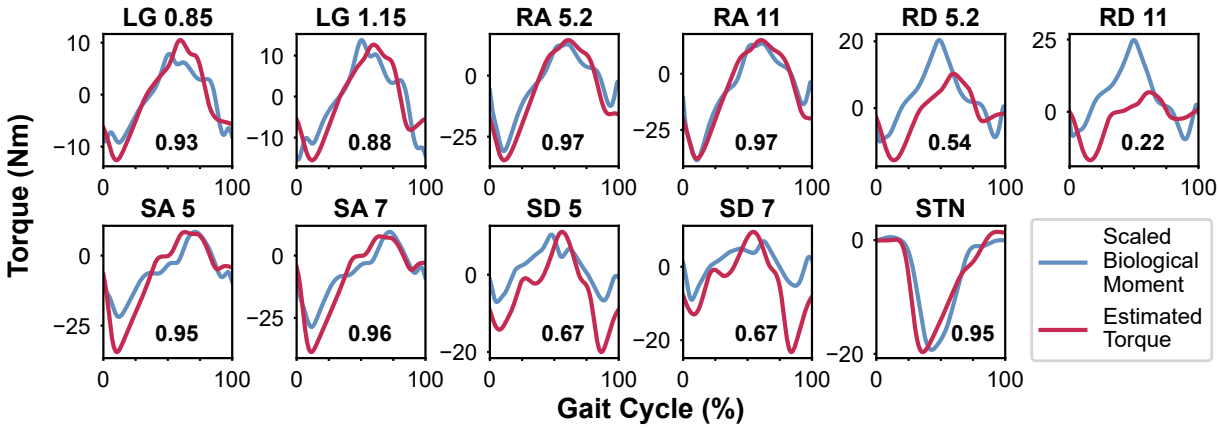

Fig. 3. *In silico* comparison between controller estimated torque and scaled biological hip moment. Estimated torque is computed using across-subject average kinematics with optimized parameters, and biological moment is the average hip moment scaled to 35%. Activities include LG (level-ground walking) at 0.85 and 1.15 m/s, RA (ramp ascent) and RD (ramp descent) on 5.2° and 11° ramps, SA (stairs ascent) and SD (stairs descent) on 5 and 7-inch step height stairs, and standing. Bold numbers in the subfigures denote the cosine similarity between the estimated torque and the scaled hip moment for the corresponding task [23].

Before the tests, participants underwent an acclimation session in which they performed different activities with the exoskeleton under different levels of assistance (LoA) until they were confident with the device. Participants also indicated the maximum LoA that they felt comfortable with across activities, which was used later in the test. To investigate the effect of exoskeleton assistance the test was performed under the following conditions: no exoskeleton (No-Exo), passive exoskeleton (0% Exo), 50% active exoskeleton (50% Exo), and 100% active exoskeleton (100% Exo), where 100% denotes the maximum comfortable LoA indicated during acclimation. Note that in the No-Exo condition, participants wore a low-profile data collection setup, with IMUs attached to body segments using elastic straps to measure kinematics.

In the multi-activity test, participants performed ADLs including level-ground walking (LG), ramp ascent (RA), ramp descent (RD), stairs ascent (SA), stairs descent (SD), sit-to-stand (STN), and stand-to-sit (SIT) on a multi-terrain circuit comprising a 3.7-m ramp inclined at 15°, a short level platform of 2 m, and a 5-step staircase with 7-inch (18 cm) step height. We repeated each activity multiple times until obtaining at least 10 gait/task cycles with average speeds within ±10% of their baseline values measured during the acclimation. Pain and difficulty were assessed using a modified Western Ontario and McMaster Universities Arthritis Index (WOMAC) questionnaire, in which participants rated their perceived pain and difficulty on a scale of 0-4, corresponding to "None", "Slight", "Moderate", "Very", and "Extremely". Additionally, participants performed a 10-meter walk test (10MWT) at their comfort and fast speeds with three repetitions each, and the average of these repetitions was recorded as their comfort or fast 10MWT speed.

B. Results

Each participant's pain and difficulty ratings across activities for each condition are shown in Table I and Table II. Additionally, Fig. 4 compares the effect of the active exoskeleton on pain and difficulty with No-Exo, where the best rating out of 50% and 100% LoA was chosen for the active condition. Compared to No-Exo, the active exoskeleton reduced the across-subject average pain rating for all tasks. Similarly, average difficulty ratings were lower with the active exoskeleton for all tasks except LG.

TABLE I

PAIN RATINGS FOR ACTIVITIES UNDER DIFFERENT CONDITIONS (NO-/0%/50%/100% EXO). BOLD ENTRIES DENOTE THE BEST ACTIVE EXOSKELETON RATINGS.

Paricipant	LG	RA	RD	SA	SD	SIT	STN
S1	1/0/**0/0**	1/1/**0/0**	1/1/1/**0**	2/1/1/**0**	1/1/**0/0**	1/2/**0/0**	1/1/1/**0**
S2	1/2/1/**0**	1/0/**0/0**	1/1/**1/1**	2/2/2/**1**	2/1/**1**/2	2/3/2/**1**	2/1/**1/1**
S3	1/2/**2/2**	2/2/**2/2**	1/2/**1/1**	3/2/2/**1**	2/2/**2/2**	2/2/2/**1**	2/2/2/**1**

TABLE II

DIFFICULTY RATINGS FOR ACTIVITIES UNDER DIFFERENT CONDITIONS (NO-/0%/50%/100% EXO). BOLD ENTRIES DENOTE THE BEST ACTIVE EXOSKELETON RATINGS.

Paricipant	LG	RA	RD	SA	SD	SIT	STN
S1	0/0/**0/0**	1/1/**0/0**	1/1/1/**0**	2/1/1/**0**	2/1/**0/0**	1/2/**0**/1	1/2/**0**/1
S2	1/2/**0/0**	1/1/**0/0**	1/1/**1/1**	2/1/2/**0**	1/1/**1**/2	2/2/1/**0**	2/1/**0**/1
S3	1/2/**2/2**	2/2/**2/2**	1/2/**1/1**	2/3/2/**1**	2/2/**2**/3	1/2/**1/1**	1/2/**1**/2

The average and individual speed changes of 10MWT in the Exo conditions compared to No-Exo condition are shown in Fig. 5. Both average comfort and fast speeds in 100% Exo condition increased compared to No-Exo condition, but with large inter-participant variation.

For comfort speed 10MWT, results from three exoskeleton conditions (0%, 50%, and 100% Exo) were compared to the No-Exo condition. S1's comfort speeds were 1.55, 1.56, and 1.52 m/s in the respective exoskeleton conditions, corresponding to changes of +0.98%, +1.63%, and -0.98% compared to the No-Exo condition (1.54 m/s). S2's comfort speeds were 1.40, 1.32, and 1.79 m/s, representing changes of -0.99%, -7.06%, and +26.46% compared to the No-Exo condition (1.42 m/s). S3's comfort speeds were 1.32, 1.36,

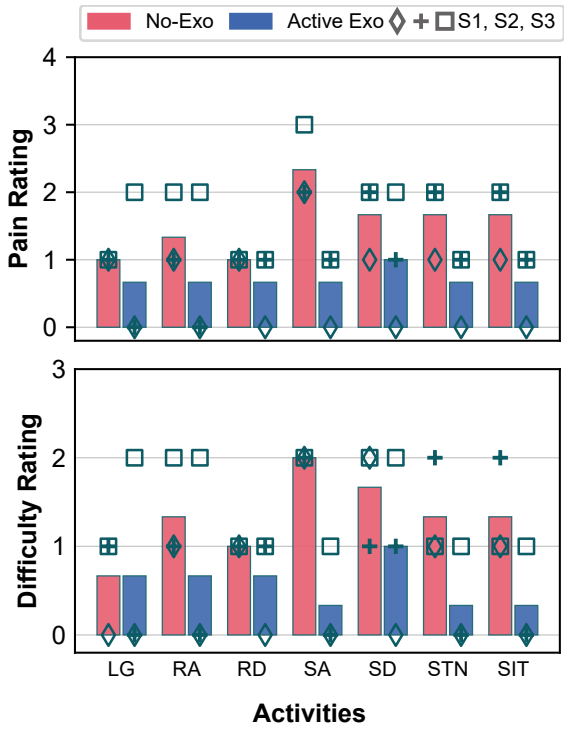

Fig. 4. Across-subject average and individual pain and difficulty ratings of activities under no exoskeleton (No-Exo) and active exoskeleton (Active Exo) conditions. Bar plots and scatter plots show the average and individual ratings.

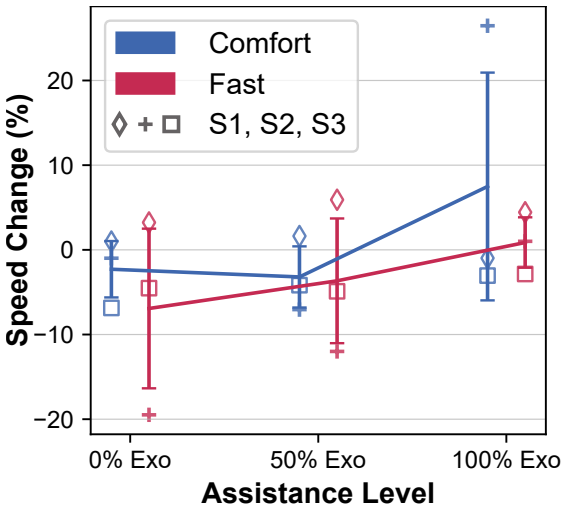

Fig. 5. Across-subject average and individual 10MWT speed changes relative to the No-Exo condition. Points where lines intersect error bars (± 1 standard deviation) indicate the mean values, and scatter plots denote individual data points. Positive numbers indicate faster speeds.

and 1.37 m/s, corresponding to changes of -6.86%, -4.17%, and -2.9% compared to the No-Exo condition (1.41 m/s).

For fast speed 10MWT, results from three exoskeleton conditions were compared to the No-Exo condition. S1's fast speeds were 1.89, 1.93, and 1.91 m/s in the respective exoskeleton conditions, corresponding to changes of +3.23%, +5.91%, and +4.44% compared to the No-Exo condition (1.83 m/s). S2's fast speeds were 1.84, 2.01, and 2.31 m/s, representing changes of -19.48%, -12.00%, and +1.01% compared to the No-Exo condition (2.28 m/s). S3's fast speeds were 1.54, 1.54, and 1.57 m/s, corresponding to changes of -4.52%, -4.89%, and -2.85% compared to the No-Exo condition (1.61 m/s).

As an exploratory result, Fig. 6 shows participants' hip joint angle over a gait cycle during 10MWT at comfort speed under No-Exo, 0% and 100% Exo conditions, overlaid with the commanded torque from the 100% Exo condition. Compared to No-Exo, hip RoM increased in 100% Exo for all participants. Specifically, the hip RoM of S1 was (-11.5°, 42.9°) in No-Exo, (-14.4°, 36.7°) in 0% Exo, and (-16.5°, 41.7°) in 100% Exo. This corresponds to 3.8° RoM increase in 100% Exo compared to No-Exo. The hip RoM of S2 was (-10.5°, 36.7°) in No-Exo, (-17.4°, 35.2°) in 0% Exo, and (-18.8°, 40.2°) in 100% Exo. This corresponds to a 11.8° RoM increase in 100% Exo compared to No-Exo. The hip RoM of S3 was (-12.0°, 40.6°) in No-Exo, (-21.2°, 30.3°) in 0% Exo, and (-22.8°, 39.3°) in 100% Exo. This corresponds to a 9.5° RoM increase in 100% Exo compared to No-Exo.

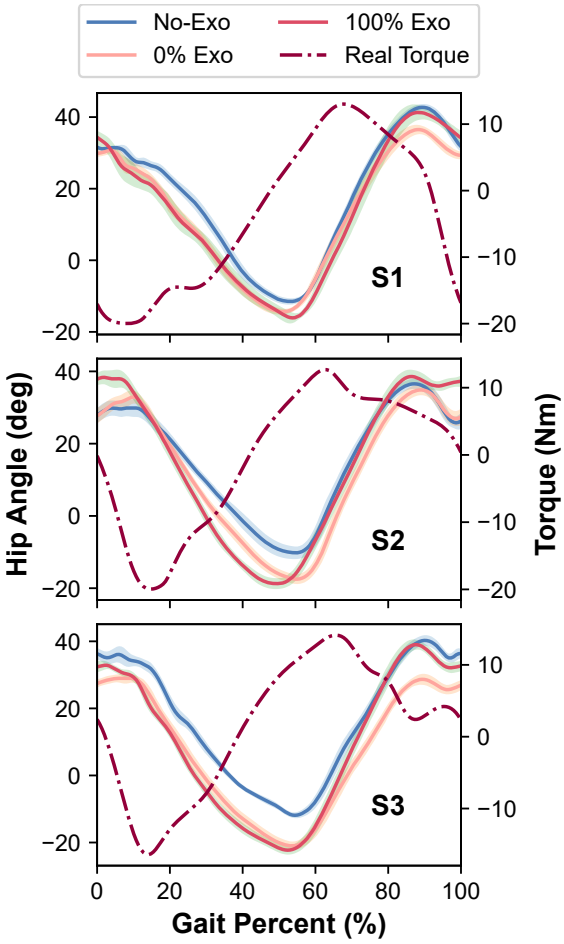

Fig. 6. Participants' hip joint angle over a gait cycle during comfortable speed 10MWT, under No-Exo, 0% Exo, and 100% Exo conditions. Solid lines represent the mean value, and shaded areas represent ±1 standard deviation. Dashed lines represent the commanded actuator torque. Positive values indicate flexion.

IV. Discussion

We hypothesized that our powered hip exoskeleton can reduce pain and difficulty in the hip OA population when performing various activities, due to reduced internal joint moments. The results of this study support our hypothesis. Across-subject pain ratings reduced across all tasks with the active exoskeleton, and the average difficulty ratings decreased for all tasks except LG. Pain and difficulty were most reduced in hip-intensive tasks like SA, STN and SIT. The small reductions in pain and difficulty in RA, an activity that requires large hip extension moment, was unexpected. A possible explanation is that participants adopted an altered gait that requires less hip effort during RA, due to muscle weakness and pain—such gait adaptations have been reported in the knee OA population during stair climbing [29]. This can also explain the lower pain/difficulty ratings in RA compared to SA in No-Exo condition. However, inverse dynamics will be needed to verify this hypothesis, which is outside the scope of this initial study.

The effect of LoA on pain and difficulty was as expected. In general, higher LoA led to the same or reduced pain and difficulty. However, for certain tasks like SD and STN, less reduction in pain or difficulty was reported in 100% Exo condition compared to other LoAs. During SD, the exoskeleton mainly does negative power, which causes resistance to leg motion, potentially leading to more difficulty. During STN, large bilateral assistive torque in the same direction needs to be applied in a short time, which leads to a large rate of torque increase. This might have increased the difficulty in 100% Exo condition, compared to milder and smoother assistive torque rates in the 50% Exo condition. The discrepancies in LoA preferences show the importance of customizability in exoskeleton control. Although we left the controller unchanged across participants in this study, the design of our controller allows user-based customization and task-specific fine-tuning to maximize the benefits of the exoskeleton in managing hip OA.

The passive exoskeleton (the 0% Exo condition) had mixed effects compared to No-Exo. In some tasks like SA, the passive exoskeleton induced benefits, likely because the underlying post-op hip brace provides hip stabilization and restricts frontal plane motions (a common strategy in OA treatment). On the other hand, increased pain and difficulty with the passive exoskeleton can still be observed in other activities, which indicates the potential penalty due to the weight and/or restrictions of the exoskeleton. Note that due to the backdrivable actuators, the penalty caused by the backdrive torque (1-2 Nm) is likely negligible. Overall, the mixed effect of the passive exoskeleton condition reflects the limited benefit of passive braces, further demonstrating the value of powered exoskeletons for OA treatment.

Slower walking speed has been observed in the hip OA population compared to the control group [30]. In this study, we compared the comfort/fast speeds during 10MWT between conditions, observing increases on average for the 100% Exo condition compared to No-Exo condition. However, large inter-subject variation exists: S1 and S2 responded well to active exoskeleton and had increases in both comfort and fast speed, while S3 did not have any speed increase with the exoskeleton. This large variability might be caused by inter-subject differences in sensorimotor factors other than muscle strength and pain; including balance, reaction time, and proprioception [31]. Although the exoskeleton can compensate for muscle strength loss and reduce pain, the assistance can also cause disruption of underlying physiology and negatively affect their gait. Therefore, acclimation is usually required for exoskeleton users to experience the most benefit. However, becoming fully acclimated to exoskeletons takes several hours, and older age further slows motor adaptation to walking with exoskeletons [32]. Therefore, it is possible that the senior most participant in our cohort (S3) did not fully acclimate to the exoskeleton, although they indicated confidence during acclimation. This may have prevented them from benefiting more from assistance compared to the younger participants.

Reduced hip RoM is a typical gait characteristic of the hip OA population during walking. This compromised gait may lead to abnormal joint load patterns at the hip and other lower extremity joints, further causing joint degeneration and chronic pain [33]. In this study, the active exoskeleton condition was associated with notably higher hip RoM compared to No-Exo. The most probable reason is the effect of the assistive extension torque of the active exoskeleton. This likely enabled participants to walk with a high peak hip extension by overcoming the effects of weak hip extensors and possible flexion contractures. On the other hand, pain arising from the higher joint forces associated with a larger step length could lead to a reduced hip RoM. The force and pain reduction capabilities of the active exoskeleton could have offset these effects, thereby encouraging larger steps and RoM. While hip RoM and walking speed are generally correlated, S1 and S3 had larger RoM despite slower speed in the 100% Exo condition. This indicates that the holistic increase in hip RoM is not simply a by-product of changes in walking speed.

The effect of the exoskeleton's assistance is evident in the commanded torque shown in Fig. 6. Across all participants, significant extension torque was provided during early-to-mid stance, which can compensate for the decreased hip extension moment associated with OA. It is important to note that normative extension torque during slow walking is typically small compared to hip-intensive activities such as ramp or stair ascent. As a result, a purely data-driven controller based on normative data would likely generate insufficient extension torque for hip OA populations, who require greater extension assistance than healthy individuals. In contrast, our controller produced large extension torques, with peak values approaching 20 Nm (the maximum allowable torque), demonstrating its ability to assist impaired populations without relying on population-specific data.

V. Conclusion

In this paper, we presented a novel biomechanics-informed, task-agnostic hip exoskeleton controller designed to address hip OA-related mobility challenges. Inspired by energy shaping principles, the controller utilizes virtual springs modulated by joint kinematics, allowing improved customizability. A pilot study with three hip OA patients showed that our hip exoskeleton and controller can reduce pain and difficulty across activities, increase hip RoM during walking, and improve 10MWT speed on an individual basis. These promising results suggest that hip exoskeletons may provide a novel conservative intervention for managing hip OA to improve patient mobility and quality of life.

Acknowledgment

The authors thank Emily Keller for assisting experiments.

References

[1] B. S. Ferket, Z. Feldman, J. Zhou, E. H. Oei, S. M. Bierma-Zeinstra, and M. Mazumdar, "Impact of total knee replacement practice: cost effectiveness analysis of data from the osteoarthritis initiative," *BMJ*, vol. 356, 2017.

[2] T. Towheed, L. Maxwell, M. Judd, M. Catton, M. C. Hochberg, and G. A. Wells, "Acetaminophen for osteoarthritis," *Cochrane database of systematic reviews*, no. 1, 2006.

[3] K. L. Bennell, D. J. Hunter, and R. S. Hinman, "Management of osteoarthritis of the knee," *BMJ*, vol. 345, 2012.

[4] M. Henriksen, E. B. Simonsen, T. Alkjær, H. Lund, T. Graven-Nielsen, B. Danneskiold-Samsøe, and H. Bliddal, "Increased joint loads during walking–a consequence of pain relief in knee osteoarthritis," *The Knee*, vol. 13, no. 6, pp. 445–450, 2006.

[5] O. A. Uthman, D. A. Van Der Windt, J. L. Jordan, K. S. Dziedzic, E. L. Healey, G. M. Peat, and N. E. Foster, "Exercise for lower limb osteoarthritis: systematic review incorporating trial sequential analysis and network meta-analysis," *BMJ*, vol. 347, 2013.

[6] J. M. Hootman, S. FitzGerald, C. A. Macera, and S. N. Blair, "Lower extremity muscle strength and risk of self-reported hip or knee osteoarthritis," *J. Physical Activity and Health*, vol. 1, no. 4, pp. 321–330, 2004.

[7] T. B. Birmingham, K. A. Marriott, K. M. Leitch, R. F. Moyer, A. L. Lorbergs, D. M. Walton, K. Willits, R. B. Litchfield, A. Getgood, P. J. Fowler *et al.*, "Association between knee load and pain: within-patient, between-knees, case–control study in patients with knee osteoarthritis," *Arthritis care & Res.*, vol. 71, no. 5, pp. 647–650, 2019.

[8] D. Hurwitz, C. Hulet, T. Andriacchi, A. Rosenberg, and J. Galante, "Gait compensations in patients with osteoarthritis of the hip and their relationship to pain and passive hip motion," *J. Orthopaedic Res.*, vol. 15, no. 4, pp. 629–635, 1997.

[9] J. Dekker, P. Tola, G. Aufdemkampe, and M. Winckers, "Negative affect, pain and disability in osteoarthritis patients: the mediating role of muscle weakness," *Behav. Res. Ther.*, vol. 31, no. 2, pp. 203–206, 1993.

[10] N. Shiba, Y. Tagawa, Y. Nakashima, S. Matsuo, K. Yamamoto, Y. Watanabe, F. Higuchi, and A. Inoue, "Biomechanical effect and clinical application of the hip joint moment reduction brace," *Clinical Orthopaedics and Related Research®*, vol. 351, pp. 149–157, 1998.

[11] A. Nérot and M. Nicholls, "Clinical study on the unloading effect of hip bracing on gait in patients with hip osteoarthritis," *Prosthetics and Orthotics Int.*, vol. 41, no. 2, pp. 127–133, 2017.

[12] E. Squyer, D. L. Stamper, D. T. Hamilton, J. A. Sabin, and S. S. Leopold, "Unloader knee braces for osteoarthritis: do patients actually wear them?" *Clinical Orthopaedics and Related Res.*, vol. 471, no. 6, pp. 1982–1991, 2013.

[13] T. G. Sutlive, H. P. Lopez, D. E. Schnitker, S. E. Yawn, R. J. Halle, L. T. Mansfield, R. E. Boyles, and J. D. Childs, "Development of a clinical prediction rule for diagnosing hip osteoarthritis in individuals with unilateral hip pain," *J. Orthopaedic & Sports Physical Therapy*, vol. 38, no. 9, pp. 542–550, 2008.

[14] R. L. Medrano, E. J. Rouse, and G. C. Thomas, "Biological joint loading and exoskeleton design," *IEEE Trans. Med. Robot. and Bionics*, vol. 3, no. 3, pp. 847–851, 2021.

[15] D. D. Molinaro, I. Kang, and A. J. Young, "Estimating human joint moments unifies exoskeleton control, reducing user effort," *Sci. Robot.*, vol. 9, no. 88, p. eadi8852, 2024.

[16] N. V. Divekar, G. C. Thomas, A. R. Yerva, H. B. Frame, and R. D. Gregg, "A versatile knee exoskeleton mitigates quadriceps fatigue in lifting, lowering, and carrying tasks," *Sci. Robot.*, vol. 9, no. 94, p. eadr8282, 2024.

[17] D. A. Winter, *Biomechanics and motor control of human movement*. John Wiley & Sons, Ltd, 2009.

[18] I. Kang, D. D. Molinaro, S. Duggal, Y. Chen, P. Kunapuli, and A. J. Young, "Real-time gait phase estimation for robotic hip exoskeleton control during multimodal locomotion," *IEEE robotics and automation letters*, vol. 6, no. 2, pp. 3491–3497, 2021.

[19] D.-S. Kim, H.-J. Lee, S.-H. Lee, W. H. Chang, J. Jang, B.-O. Choi, G.-H. Ryu, and Y.-H. Kim, "A wearable hip-assist robot reduces the cardiopulmonary metabolic energy expenditure during stair ascent in elderly adults: a pilot cross-sectional study," *BMC geriatrics*, vol. 18, pp. 1–8, 2018.

[20] C. McGibbon, A. Sexton, A. Jayaraman, S. Deems-Dluhy, E. Fabara, C. Adans-Dester, P. Bonato, F. Marquis, S. Turmel, and E. Belzile, "Evaluation of a lower-extremity robotic exoskeleton for people with knee osteoarthritis," *Assistive Technol.*, vol. 34, no. 5, pp. 543–556, 2022.

[21] J. Lin, N. V. Divekar, G. C. Thomas, and R. D. Gregg, "Optimally biomimetic passivity-based control of a lower-limb exoskeleton over the primary activities of daily life," *IEEE Open J. Control Syst.*, vol. 1, pp. 15–28, 2022.

[22] K. Walters, G. C. Thomas, J. Lin, and R. D. Gregg, "An energetic approach to task-invariant ankle exoskeleton control," in *IEEE/RSJ Int. Conf. on Intelligent Robots and Syst. (IROS)*, 2023, pp. 6082–6089.

[23] J. Zhang, J. Lin, V. Peddinti, and R. D. Gregg, "Optimal energy shaping control for a backdrivable hip exoskeleton," in *2023 Amer. Control Conf. (ACC)*. IEEE, 2023, pp. 2065–2070.

[24] J. Lin, G. C. Thomas, N. V. Divekar, V. Peddinti, and R. D. Gregg, "A modular framework for task-agnostic, energy shaping control of lower limb exoskeletons," *IEEE Trans. Control Syst. Technol.*, vol. 32, no. 6, pp. 2359–2375, 2024.

[25] J. Lin, N. Divekar, G. Lv, and R. D. Gregg, "Energy shaping control with virtual spring and damper for powered exoskeletons," in *2019 IEEE 58th Conference on Decision and Control (CDC)*, 2019, pp. 3039–3045.

[26] B. Laschowski, R. Sharif Razavian, and J. McPhee, "Measurement and simulation of human sitting and standing movement biomechanics," 2019. [Online]. Available: https://dx.doi.org/10.21227/9cqv-w712

[27] J. Camargo, A. Ramanathan, W. Flanagan, and A. Young, "A comprehensive, open-source dataset of lower limb biomechanics in multiple conditions of stairs, ramps, and level-ground ambulation and transitions," *J. Biomech.*, vol. 119, p. 110320, 2021.

[28] C. Nesler, G. Thomas, N. Divekar, E. J. Rouse, and R. D. Gregg, "Enhancing voluntary motion with modular, backdrivable, powered hip and knee orthoses," *IEEE Robot. and Automat. Lett.*, vol. 7, no. 3, pp. 6155–6162, 2022.

[29] J. L. Asay, A. Mündermann, and T. P. Andriacchi, "Adaptive patterns of movement during stair climbing in patients with knee osteoarthritis," *J. Orthopaedic Research*, vol. 27, no. 3, pp. 325–329, 2009.

[30] D. Schmitt, A. Vap, and R. M. Queen, "Effect of end-stage hip, knee, and ankle osteoarthritis on walking mechanics," *Gait & posture*, vol. 42, no. 3, pp. 373–379, 2015.

[31] M. L. Callisaya, L. Blizzard, M. D. Schmidt, J. L. McGinley, S. R. Lord, and V. K. Srikanth, "A population-based study of sensorimotor factors affecting gait in older people," *Age and Ageing*, vol. 38, no. 3, pp. 290–295, 2009.

[32] A. Lakmazaheri, S. Song, B. B. Vuong, B. Biskner, D. M. Kado, and S. H. Collins, "Optimizing exoskeleton assistance to improve walking speed and energy economy for older adults," *J. NeuroEng. and Rehabil.*, vol. 21, no. 1, p. 1, 2024.

[33] M. Murray, D. R. Gore, and B. Clarkson, "Walking patterns of patients with unilateral hip pain due to osteo-arthritis and avascular necrosis," *JBJS*, vol. 53, no. 2, pp. 259–274, 1971.